Circulation Research

Check for updates

ORIGINAL RESEARCH

Calpain-Dependent Protein Degradation Contributes to CASQ2-R33Q CPVT

Laura Ramos-Hernández, Demetrio J. Santiago, Rocío F. Serrano-Blanco, Andrea Cancemi, Lorena Esteban-Martínez, Emilio Camafeita, Marina López-Olañeta, Deni Kukavica, Ana Guío-Carrión, Jesús M. Vázquez, Miguel Torres, Silvia G. Priori, Enrique Lara-Pezzi

BACKGROUND: Catecholaminergic polymorphic ventricular tachycardia (CPVT) is an inherited arrhythmogenic disease associated with cardiac arrest in children and young adults. The recessive form of CPVT is caused by loss-of-function mutations in the genes encoding CASQ2 (calsequestrin 2) and TRDN (triadin), which, together with JCTN (junctin), regulate the release of calcium ions from the sarcoplasmic reticulum through the RyR2 (ryanodine receptor). The *CASQ2* R33Q mutation causes calcium mishandling and ventricular tachycardia through triggered activity. The homozygous mouse model *Casq2*$^{R33Q/R33Q}$ closely replicates the clinical phenotype of patients with CPVT. In this model, CASQ2, TRDN, and JCTN levels are markedly reduced; however, the mechanisms underlying this reduction and their contribution to CPVT are incompletely understood.

METHODS: We used a combination of proteomics, animal models, and experimental methods to identify the molecular mechanisms responsible for the decrease of couplon proteins in *Casq2*$^{R33Q/R33Q}$ mice and to explore their functional contribution to the disease.

RESULTS: *Casq2*$^{R33Q/R33Q}$ hearts showed activation of endoplasmic reticulum stress, the unfolded protein response, and alterations in major proteolytic pathways. Inhibition of the proteasome or autophagy in neonatal cardiomyocytes and adult mice partially restored CASQ2 but not TRDN levels, suggesting distinct degradation mechanisms. In contrast, calpain inhibition restored CASQ2 and TRDN protein levels, decreased triggered activity in isolated cardiomyocytes, and reduced ventricular tachycardia episodes in vivo in *Casq2*$^{R33Q/R33Q}$ mice. Biochemical assays showed that TRDN is a direct calpain substrate. TRDN degradation preceded CASQ2 loss, and TRDN overexpression using modified RNA in cardiomyocytes or an adeno-associated viral vector in vivo increased CASQ2 levels in mutant mice, supporting an upstream role for TRDN destabilization.

CONCLUSIONS: Couplon protein loss in CPVT associated with CASQ2-R33Q is mediated by coordinated but distinct proteolytic pathways, with calpain-dependent TRDN degradation representing a key pathogenic event that promotes CASQ2 destabilization and arrhythmogenesis.

GRAPHIC ABSTRACT: A graphic abstract is available for this article.

Key Words: autophagy ■ calpain ■ endoplasmic reticulum stress ■ myocytes, cardiac ■ tachycardia

Meet the First Author, see p e000772 | Editorial, see Article by Do and Knollmann

Catecholaminergic polymorphic ventricular tachycardia (CPVT) is an inherited arrhythmogenic heart syndrome mainly affecting children and young adults.[1] It is characterized by life-threatening arrhythmias triggered by physical or emotional stress that can cause syncope or sudden death in the absence of structural heart disease and with a normal resting ECG.[2,3]

The underlying cause of CPVT is attributed to mutations in different genes encoding proteins that control Ca^{2+} release from the sarcoplasmic reticulum (SR) in

Correspondence to: Enrique Lara-Pezzi, PhD, Myocardial Homeostasis and Cardiac Injury Programme, Centro Nacional de Investigaciones Cardiovasculares (CNIC), Melchor Fernandez Almagro, 3, Madrid 28029, Spain, Email elara@cnic.es; or Silvia G. Priori, MD, PhD, Molecular Cardiology Unit, IRCCS Istituti Clinici Scientifici Maugeri, Via S Maugeri, 10, Pavia 27100, Italy, Email silvia.priori@icsmaugeri.it

Supplemental Material is available at https://www.ahajournals.org/doi/suppl/10.1161/CIRCRESAHA.126.329035.

© 2026 The Authors. *Circulation Research* is published on behalf of the American Heart Association, Inc., by Wolters Kluwer Health, LLC. This is an open access article under the terms of the Creative Commons Attribution Non-Commercial-NoDerivs License, which permits use, distribution, and reproduction in any medium, provided that the original work is properly cited, the use is noncommercial, and no modifications or adaptations are made.

Circulation Research is available at www.ahajournals.org/journal/res

Downloaded from http://ahajournals.org by on November 5, 2026

ORIGINAL RESEARCH

Downloaded from http://ahajournals.org by on November 5, 2026

Novelty and Significance

What Is Known?

- Catecholaminergic polymorphic ventricular tachycardia caused by recessive *CASQ2* mutations is associated with defective sarcoplasmic reticulum Ca^{2+} handling and stress-induced ventricular arrhythmias.
- In the *CASQ2* R33Q mutation model, myocardial levels of CASQ2 (calsequestrin 2), TRDN (triadin), and JCTN (junction) are markedly reduced despite preserved transcript expression.
- The molecular pathways responsible for couplon protein loss and their contribution to arrhythmogenesis were previously unclear.

What New Information Does This Article Contribute?

- *CASQ2* R33Q mutation hearts show activation of endoplasmic reticulum stress, unfolded protein response signaling, and multiple proteolytic pathways.
- CASQ2 degradation is mediated mainly by proteasomal and autophagic pathways, whereas TRDN is a direct substrate of calpain, and its loss precedes CASQ2 destabilization.
- Pharmacological calpain inhibition restores couplon protein levels, improves triggered activity, and reduces ventricular tachycardia, identifying calpain as a therapeutic target in catecholaminergic polymorphic ventricular tachycardia.

Catecholaminergic polymorphic ventricular tachycardia is caused by defects in the machinery that controls calcium release in heart muscle cells, but how these defects lead to further disruption of this machinery is not fully understood. Here, we show that abnormal calcium handling caused by mutant calsequestrin activates cellular protein-degradation pathways that further destabilize the calcium-release complex. A key event in this process is activation of calpain, which directly degrades triadin, a protein that helps organize and stabilize this complex. Loss of triadin precedes and promotes the loss of mutant calsequestrin, revealing an unexpected sequence of events in the progression of the original molecular defect. Importantly, inhibiting calpain restores several components of the calcium-release machinery, improves calcium handling in heart muscle cells, and reduces ventricular arrhythmias in mice. These findings identify activation of protein degradation as an additional disease mechanism that can amplify the consequences of abnormal calcium handling. More broadly, they suggest that protecting the stability of the cardiac calcium-release machinery may provide a new therapeutic strategy for inherited arrhythmias.

Nonstandard Abbreviations and Acronyms

α-fodrin	alpha-fodrin
AAV	adeno-associated virus
ATF	activating transcription factor
CAPN1	calpain 1
CASQ2	calsequestrin 2
CNX	Ca2+-binding protein calnexin
CPVT	catecholaminergic polymorphic ventricular tachycardia
ER	endoplasmic reticulum
ERAD	endoplasmic reticulum–associated degradation
GFP	green fluorescent protein
GRP	glucose-regulated protein
HRC	histidine-rich calcium-binding protein
ISG15	interferon-stimulated gene 15
JCTN	junctin
LAMP1	lysosome-associated membrane glycoprotein 1
MYBPC3	myosin-binding protein C3
PLN	phospholamban
P-PLN	PLN phosphorylation
PSMD	proteasome 26S subunit ubiquitin receptor non-ATPase
RyR2	ryanodine receptor 2
SERCA2a	sarcoplasmic/endoplasmic reticulum calcium ATPase 2a
SR	sarcoplasmic reticulum
SRL	sarcalumenin
TOLLIP	toll-interacting protein
TRDN	triadin
TTN	titin
UPS	ubiquitin-proteasome system
VT	ventricular tachycardia
WT	wild-type

cardiomyocytes.[2] Activation of β-adrenergic receptors by catecholamines released during stress or exercise in these patients results in pathological SR Ca^{2+} release during diastole, Ca^{2+}-triggered action potentials, and ventricular tachycardia (VT) episodes.[1,3]

Typical CPVT is caused by pathogenic variants in genes encoding couplon proteins, mainly in *RYR2* and

CASQ2, which account for ≈70% and 5% of all CPVT cases, respectively.[1,3] The cardiomyocyte couplon coordinates proteins that jointly regulate SR Ca^{2+} release during systole. RyR2 (ryanodine receptor 2) forms a homotetrameric calcium-release channel on the junctional SR membrane and is the main mediator of Ca^{2+}-induced Ca^{2+} release in cardiomyocytes.[4] CASQ2 (calsequestrin 2), located in the SR lumen, functions both as an intracellular Ca^{2+} buffer within the SR and as a modulator of the sensitivity of RyR2 to luminal Ca^{2+}. TRDN (triadin) and JCTN (junctin) act as scaffold proteins in the SR membrane, anchoring CASQ2 to RyR2.[5–7]

The most common form of CPVT is autosomal dominant, caused by gain-of-function mutations in *RYR2*.[8] Missense pathogenic variants in *CASQ2* cause a recessive, but clinically more aggressive form of the disease, although certain heterozygous patients may also manifest the disease phenotype.[9] Mutations in TRDN have also been linked to the development of CPVT, albeit the prevalence is much lower.[10]

A mouse model bearing the R33Q recessive mutation in *CASQ2* reproduces human CPVT caused by this same mutation.[11] *Casq2*$^{R33Q/R33Q}$ homozygous mutant mice develop VT episodes on exposure to environmental stress, with reduced SR Ca^{2+} content in cardiomyocytes and adrenergic receptor–mediated delayed afterdepolarizations and early afterdepolarizations leading to triggered activity. Expression of wild-type (WT) CASQ2 in *CASQ2* null and mutant knock-in mice with an adeno-associated viral (AAV) vector improved the pathological phenotype.[3,12] Importantly, *Casq2*$^{R33Q/R33Q}$ mice show decreased content of CASQ2, TRDN, and JCTN proteins, with no changes in mRNA expression.[11] However, the mechanisms underlying the downregulation of couplon proteins and their potential impact on the development of CPVT are incompletely understood.

In this work, we identified the main processes responsible for the degradation of CASQ2, TRDN, and JCTN in *Casq2*$^{R33Q/R33Q}$ mice. We show that CASQ2 and JCTN are degraded in response to endoplasmic reticulum (ER) stress through the proteasome, whereas TRDN is degraded by calpain. Importantly, proteasome inhibition recovered CASQ2 but not TRDN levels. In contrast, calpain inhibition resulted in increased expression of all couplon proteins and reduced VT episodes. These results shed light on the molecular mechanisms mediating the development of CPVT and pave the way for new therapeutic approaches based on the inhibition of couplon protein degradation.

METHODS

Data Availability

The proteomics data generated in this study have been deposited in the jPOST repository under accession number JPST004689. Other data that support the findings of this study are available from the corresponding author on reasonable request. Descriptions of additional experimental procedures and materials are provided in the Supplemental Methods. Key experimental resources are listed in the Major Resources Table in the Supplemental Material.

Mice

The homozygous *Casq2*$^{R33Q/R33Q}$ knock-in strain was generated by homologous recombination using genetic manipulation of embryonic stem cells.[11] Homozygous *Casq2* null (*Casq2*$^{-/-}$) mice were also chosen because of their extensively expressed phenotypic manifestations of CPVT.[13] C57BL/6NCrL mice from Charles River Laboratories were designated *Casq2*$^{WT/WT}$ and used as WT controls. Experiments were performed in 2-month-old adult mice and in 1-day-old (P1) neonatal mice. Because no consistent sex-dependent differences have been described in patients with CPVT or in mouse models of CPVT associated with CASQ2 variants, pooled data from both sexes were used, as previously described in this model.[12] Neonatal mice were euthanized by decapitation, and adult mice were euthanized by cervical dislocation. Animals were maintained and studied according to the protocols approved by the local ethics committee of the Spanish National Center for Cardiovascular Research and the Regional Government of Madrid (PROEX 177/17 and PROEX 191.5/22). Power calculations were performed to determine the required number of animals based on previous data (P=0.05; power=80%).

For pharmacological treatment, *Casq2*$^{WT/WT}$ and *Casq2*$^{R33Q/R33Q}$ 2-month-old mice were randomized to different treatment groups using simple randomization. Drugs were administered by intraperitoneal injection. Flecainide (20 mg/kg; Focus Biomolecules) was administered every 12 hours for 3 consecutive days. Proteasome activity was inhibited with bortezomib (1 mg/kg; MedChemExpress) once daily for 3 consecutive days. For autophagy inhibition, mice were treated with a single dose of hydroxychloroquine sulphate (50 mg/kg; Sigma) for 24 hours. For calpain inhibition, MDL28170 (70 mg/kg; MedChemExpress) or calpeptin (20 mg/kg; Sigma-Aldrich CAS 117591-20-5) was administered once daily for 3 consecutive days. At the end of the treatment, mice were euthanized, and myocardial proteins were extracted.

For AAV administration, 7×10^{10} viral particles of AAV-TRDN and AAV-EGFP (enhanced GFP) were injected into the femoral vein of 2-month-old mice after simple randomization. In both AAV vectors, TRDN and EGFP were expressed under the control of the TnT (Troponin T) promoter. Vectors were packaged into an AAVmyo capsid. Mice were euthanized 4 weeks later, and myocardial proteins were extracted.

Neonatal Cardiomyocytes Isolation and Treatment

Cardiomyocytes were isolated from *Casq2*$^{WT/WT}$ and *Casq2*$^{R33Q/R33Q}$ newborn mice (1 day after birth, P1), as previously described by our group.[14] Briefly, hearts were removed from the newborn mice on the day of birth. Sequential, partial digestions were performed with type 2 collagenase (LS004176, Worthington) until the hearts were completely digested, and the isolated cells were stored in fetal bovine serum. Cells were seeded in 10 cm^2 plates pretreated with 1% gelatin and maintained in Dulbecco's modified Eagle's medium (DMEM) supplemented with 20% 199 medium, 15% fetal bovine serum, 15% HEPES (4-[2-hydroxyethyl]-1-piperazineethanesulfonic acid) and 2 mmol/L L-glutamine.

Downloaded from http://ahajournals.org by on November 5, 2026

For pharmacological treatment, neonatal cardiomyocytes were isolated and seeded in a 24-well plate in 0.5 mL of culture medium supplemented as described above. The next day, cells were treated with different proteolytic inhibitors or the corresponding vehicle. Protein synthesis was blocked by treating neonatal cardiomyocytes with cycloheximide (Sigma) at 50 µM for 2, 4, and 8 hours. Flecainide (Focus Biomolecules) was used at 20 µM for 8 hours. For proteasome and ER-associated degradation (ERAD) inhibition, cells were exposed to MG132 (Sigma) and eeyarestatin (Sigma), respectively, at 10 µM for 8 hours. Autophagy was inhibited with hydroxychloroquine (Sigma) at 30 µM for 8 hours. To inhibit calpain, cells were treated with calpeptin (Abcam) at 10 µM for 8 hours. At the end of the treatment, cells were harvested, and proteins were extracted and analyzed as described below.

ECG Recording by Telemetry

Mice were anesthetized with 3% to 3.5% sevoflurane administered with 100% oxygen, and the telemetry device (Data Sciences International) was implanted subcutaneously in their back. Baseline ECGs were recorded for 5 minutes. Epinephrine (2 mg/kg; B. Brown) was injected intraperitoneally, and ECGs were recorded for a further 20 minutes. ECG data acquisition was performed using the Ponemah software (Data Sciences International). Both acquisition and analysis of ECG data were performed by a blinded operator.

Statistical Analysis

Normality was assessed using the D'Agostino-Pearson test. The vast majority of the subgroups successfully passed the normality threshold. For subgroups showing mild deviations from normality, an ordinary 2-way ANOVA was still used, considering the robust nature of a balanced factorial design against minor distribution violations. For quantitative values, the Mann-Whitney *U* test was used to compare means of 2 groups for a single time point. Two-way ANOVA with an appropriate posttest was used to compare multiple conditions with 2 variables, as indicated in the figure legends. Categorical variables were analyzed using contingency tables with the Fisher exact test. Changes were considered statistically significant if $P<0.05$. GraphPad Prism 8.0.1 and R version 4.5.2 were used to perform all the statistical analyses and graphs. Additional statistical methods for the proteomics analysis are provided in the Supplemental Material.

RESULTS

Changes in Protein Expression and Posttranslational Modification in *Casq2*$^{R33Q/R33Q}$ Mice

To investigate the molecular mechanisms underlying the detrimental effects of the CASQ2-R33Q mutation, proteomics analysis was performed on adult *Casq2*$^{WT/WT}$ and *Casq2*$^{R33Q/R33Q}$ mouse hearts (Figure 1A through 1F). Mutant mice showed downregulation of several calcium-handling proteins in the SR, including CASQ2, TRDN, JCTN/*ASPH* (Aspartate Beta-Hydroxylase), and SRL (sarcalumenin), as well as increased expression of HRC (histidine-rich calcium-binding protein), which competes with CASQ2 to bind RyR2. Overall, the results showed a mild decrease in proteins related to myocardial contraction and the electron transport chain, together with an increase in proteins associated with inflammation, glycolysis, protein synthesis and oligomerization, and the proteasome complex (Figure 1A and 1C; Table S1). Specifically, *Casq2*$^{R33Q/R33Q}$ mice showed an upregulation of proteins associated with protein degradation, including TOLLIP (toll-interacting protein), the ubiquitin-like protein ISG15 (interferon-stimulated gene 15), the lysosomal protein LAMP1 (lysosome-associated membrane glycoprotein 1), and PSMD2 (proteasome 26S subunit ubiquitin receptor non-ATPases 2) and PSMD11. Furthermore, mutant mice showed increased levels of ER chaperones required for protein folding and quality control, including GRP94 (glucose-regulated protein 94), GRP78, and CNX (calnexin), a Ca^{2+}-binding protein, suggesting activation of ER stress (Figure 1A and 1C). Interestingly, no upregulation of ER stress markers was observed in CASQ2-knockout mice (Figure 1B and 1D). Furthermore, we found a poor correlation between protein expression changes in knockout and mutant mice, suggesting that the mechanisms leading to CPVT in different models are diverse (Figure 1E).

Because *Casq2*$^{R33Q/R33Q}$ mice showed an enrichment in the protein phosphorylation category (Figure 1C), we quantified with SanXoT the differences in protein phosphorylation between WT and mutant animals. The results showed changes in the phosphorylation of some SR Ca^{2+} regulators, including an increase in HRC (Ser96) and a decrease in SERCA2a (sarcoplasmic/endoplasmic reticulum calcium ATPase 2a; Ser38), PLN (phospholamban; Ser16 [Serine 16] and Thr17), and the chaperones HSP90AB1 (Heat shock protein 90 kDa alpha, class B, member 1; Ser287) and CNX (Ser582; Figure 1F; Table S2). In addition, changes in the phosphorylation of sarcomeric proteins TTN and MYBPC3 (myosin-binding protein C3) were detected (Figure 1F).

TRDN Degradation Precedes CASQ2 Loss and Its Restoration Rescues CASQ2 Stability

To establish the mechanisms responsible for the downregulation of couplon proteins in *Casq2*$^{R33Q/R33Q}$ mice, we first investigated their degradation rate. After cycloheximide treatment to inhibit protein translation, we found that CASQ2 half-life was significantly reduced in neonatal cardiomyocytes from *Casq2*$^{R33Q/R33Q}$ mice compared with WT controls (Figure S1A and S1B). TRDN also showed a faster decrease after cycloheximide treatment in neonatal cardiomyocytes from mutant mice (Figure S1A and S1C). Importantly, TRDN degradation rate seemed to be faster than that of CASQ2, reaching an 84% decrease by 8 hours.

To determine whether the faster degradation of TRDN might contribute to CASQ2 destabilization, we

Downloaded from http://ahajournals.org by on November 5, 2026

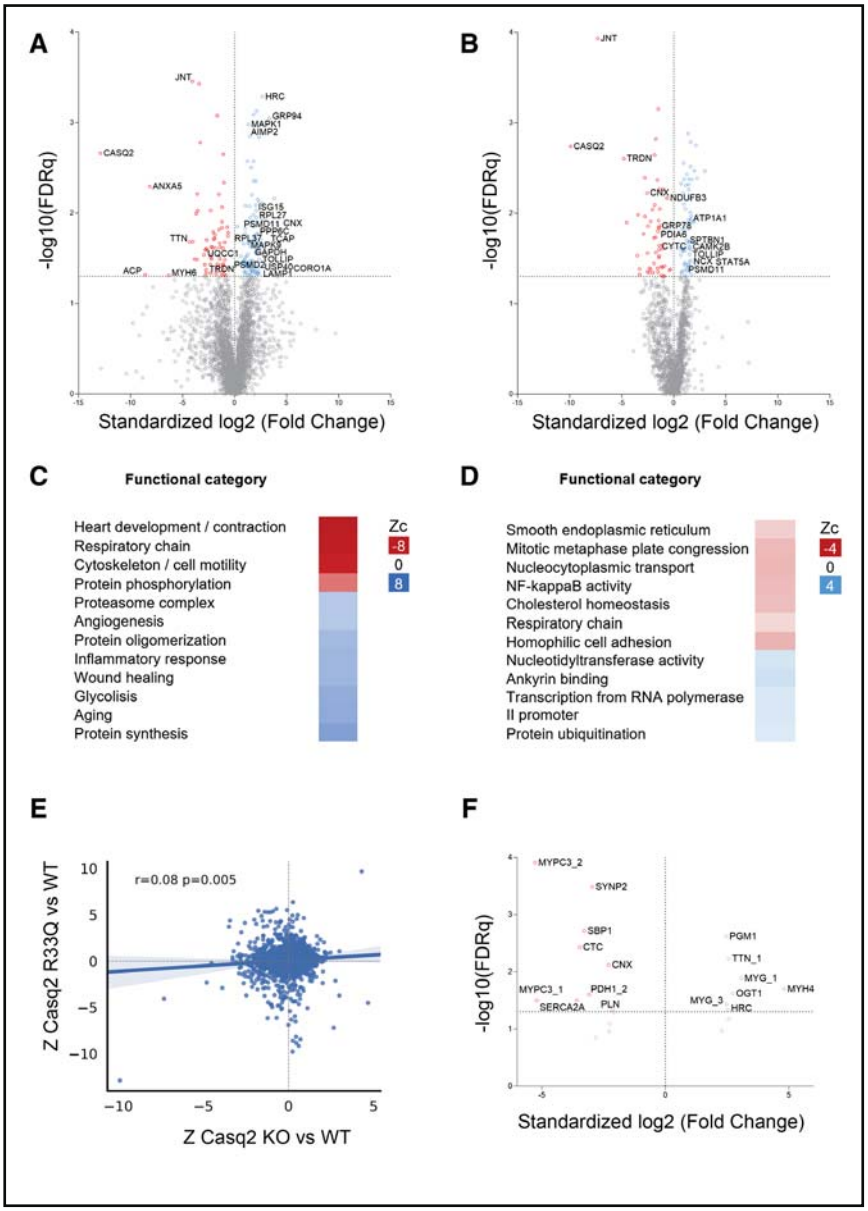


Figure 1. Proteomics analysis reveals distinct changes in *Casq2*$^{R33Q/R33Q}$ mice heart.
A and **B**, Volcano plots showing the differential proteomics profile comparing *Casq2*$^{R33Q/R33Q}$ to *Casq2*$^{WT/WT}$ (**A**) or *Casq2*$^{-/-}$ to *Casq2*$^{WT/WT}$ (**B**) hearts. The x-axis (Zq) represents the standardized log2 ratio of protein abundance between conditions, whereas the y-axis shows the −log10 of the adjusted *P* value (FDR, false discovery rate). Statistical significance was determined using SanXoT (see Supplementary Material) and defined as FDR<0.05 (corresponding to −log10[FDR]>1.3). Red and blue dots correspond to down- or upregulated proteins, respectively (*P*<0.05). Proteins that did not change significantly are represented as gray dots (*P*>0.05). **C,** Gene Ontology (GO) enrichment analysis. Functional category changes were assessed using SanXoT as described in the Supplemental Methods. The standardized variable Zc (R33Q [*Casq2*$^{R33Q/R33Q}$] *vs* WT [*Casq2*$^{WT/WT}$]) represents the coordinated change in abundance of the proteins assigned to each functional category, with positive and negative values indicating enrichment in either direction and magnitude represented by color intensity. **D,** GO enrichment analysis was performed as in (**C**) to compare knockout (KO; *Casq2*$^{-/-}$) *vs* wild-type (WT; *Casq2*$^{WT/WT}$) hearts. **E,** Regression analysis comparing *Casq2*$^{-/-}$ (KO) and *Casq2*$^{R33Q/R33Q}$ (R33Q) mice. **F,** Volcano plot showing the differential phosphoproteomics profile comparing *Casq2*$^{R33Q/R33Q}$ *vs* *Casq2*$^{WT/WT}$ mice hearts. The x-axis (Zq) represents the standardized log2 ratio of phosphopeptide abundance between conditions, whereas the y-axis shows the −log10 of the adjusted *P* value (FDR). Statistical significance was defined as FDR<0.05 (corresponding to −log10[FDR]>1.3). CASQ2 indicates calsequestrin 2; HRC, histidinerich calcium-binding protein; JCTN, junction; PLN, phospholamban; P-PLN, PLN phosphorylation; SERCA2a, sarcoplasmic/endoplasmic reticulum calcium ATPase 2a; and TRDN, triadin.

reexpressed TRDN in mutant cardiomyocytes and assessed its impact on CASQ2 levels. First, we transfected neonatal cardiomyocytes from *Casq2*$^{R33Q/R33Q}$ mice with modified RNA encoding TRDN or a GFP (green fluorescent protein) control. Western blot analysis showed that induction of TRDN expression led to increased CASQ2 protein levels in mutant cardiomyocytes (Figure S2A and S2B). To confirm these findings

Downloaded from http://ahajournals.org by on November 5, 2026

in vivo, we generated an AAV vector expressing TRDN under the control of the cardiac troponin promoter, packaged into the AAVmyo capsid. Systemic administration of AAV-TRDN to *Casq2*$^{R33Q/R33Q}$ mice resulted in elevated myocardial TRDN levels, as expected, and a parallel increase in CASQ2 expression (Figure S2C and S2D). Together, these results suggest that loss of TRDN precedes and facilitates subsequent CASQ2 degradation in *Casq2*$^{R33Q/R33Q}$ hearts.

Aberrant Calcium Handling Contributes to Couplon Protein Degradation in *Casq2*$^{R33Q/R33Q}$ Mice

To confirm the changes in calcium regulators identified by proteomics, left ventricle samples from adult *Casq2*$^{R33Q/R33Q}$ and *Casq2*$^{WT/WT}$ mice were analyzed using Western blot. Samples from *Casq2*$^{R33Q/R33Q}$ mice showed a significant increase in HRC expression and a decrease in P-PLN (PLN phosphorylation; Ser16/Thr17), with no changes in total PLN or SERCA2a levels (Figure 2A and 2B). Because reduced P-PLN results in attenuated SERCA2a activity,[15] these changes may be associated with an increased Ca^{2+} concentration in the cytosol.

The antiarrhythmic drug flecainide is a RyR2 inhibitor that reduces spontaneous SR Ca^{2+} release into the cytosol during diastole.[16] Flecainide has been shown to reduce the incidence of adverse arrhythmic events in a large cohort of patients with CPVT, especially among those who were refractory to β-blocker treatment.[17] It also prevented CPVT in a mouse model bearing the R4496C mutation

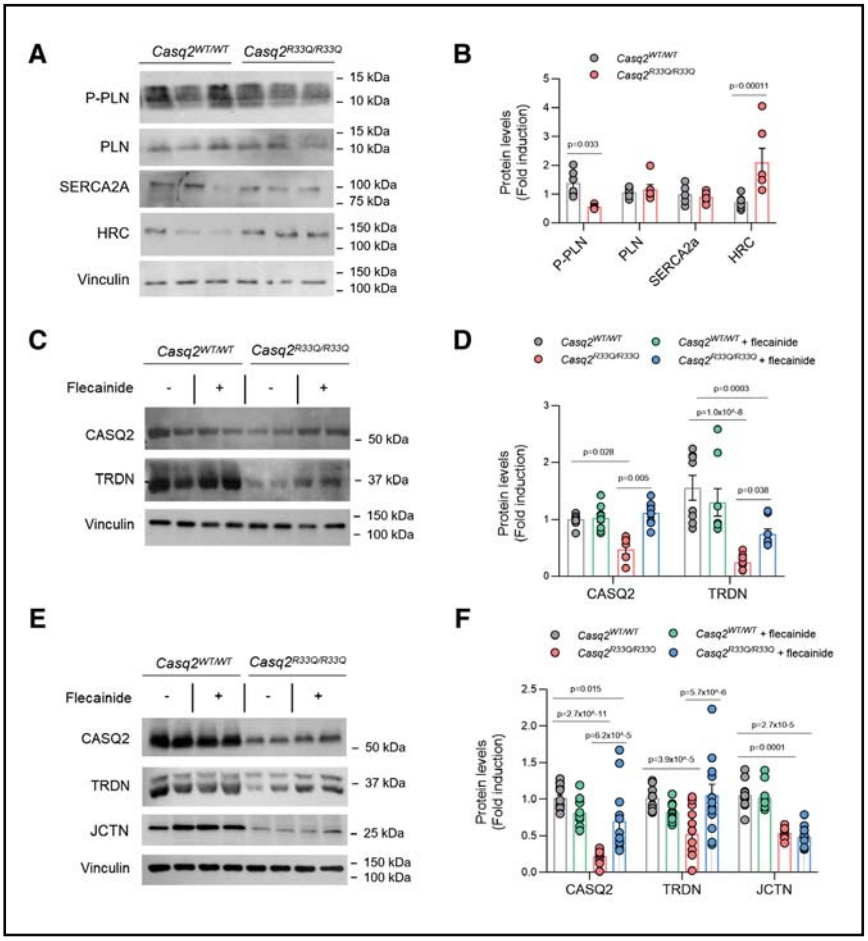


Figure 2. Calcium homeostasis regulators are altered in CASQ2 (calsequestrin 2) mutant mice.
A and **B**, Protein levels of different calcium release and uptake regulators were analyzed by Western blot (**A**), and band intensity was quantified (**B**). Vinculin was used as a loading control. Data are represented as average fold change over the values of *Casq2*$^{WT/WT}$ mice±SEM. Two-way ANOVA with Šídák multiple comparisons test was used. n=6 mice per group. **C** and **D**, Protein extracts from *Casq2*$^{R33Q/R33Q}$ and *Casq2*$^{WT/WT}$ neonatal cardiomyocytes treated or untreated with 20 µmol/L flecainide were analyzed by Western blot and quantified. Data are represented as fold induction±SEM over the values of untreated *Casq2*$^{WT/WT}$ neonatal cardiomyocytes. Two-way ANOVA with Tukey multiple comparison test was used. n=8 per group. **E** and **F**, Myocardial protein extracts from *Casq2*$^{R33Q/R33Q}$ and *Casq2*$^{WT/WT}$ mice treated or untreated with flecainide were analyzed by Western blot and quantified. Data are represented as fold induction±SEM over the values of untreated *Casq2*$^{WT/WT}$ mice. Two-way ANOVA with Tukey multiple comparison test was used. n=13 (CASQ2, TRDN) and n=10 (JCTN) per group. CASQ2 indicates calsequestrin 2; HRC, histidine-rich calcium-binding protein; JCTN, junction; PLN, phospholamban; P-PLN, PLN phosphorylation; SERCA2a, sarcoplasmic/endoplasmic reticulum calcium ATPase 2a; and TRDN, triadin.

Downloaded from http://ahajournals.org by on November 5, 2026

in RyR2 and in *CASQ2* knockout mice.[18,19] To determine whether flecainide had any effect on couplon protein stability in *Casq2*$^{R33Q/R33Q}$ mice, neonatal cardiomyocytes isolated from mutant mice were treated with flecainide for 8 hours. The results showed an increase in CASQ2 and TRDN protein levels in flecainide-treated cardiomyocytes compared with untreated cells (Figure 2C and 2D). To validate these results in vivo, 2-month-old *Casq2*$^{R33Q/R33Q}$ and *Casq2*$^{WT/WT}$ mice were injected intraperitoneally with flecainide or vehicle for 3 consecutive days. Western blot analysis showed an increase in CASQ2 and TRDN proteins in flecainide-treated *Casq2*$^{R33Q/R33Q}$ mice compared with untreated *Casq2*$^{R33Q/R33Q}$ mice, with no changes in WT mice. However, this beneficial effect was not evident with JCTN levels (Figure 2E and 2F). These results suggest that degradation of CASQ2 and TRDN in mutant mice is the result rather than the cause of Ca^{2+} mishandling, at least partially.

CASQ2 Degradation in *Casq2*$^{R33Q/R33Q}$ Mice Depends on the ERAD Pathway

Because the proteomics analysis had shown an increase in ER stress proteins in mutant mice, we explored the potential role of this pathway in the degradation of couplon proteins in CPVT. We aimed to validate the identified changes using Western blot, and we investigated additional pathways associated with ER stress. As shown in Figure 3A and 3B, *Casq2*$^{R33Q/R33Q}$ adult mice showed a significant increase in GRP94, GRP78, and CNX expression. In addition, the unfolded protein response–related transcription factors ATF6 (Activating transcription factor 6) and ATF4, and the spliced form of XBP1 (XBP1s, X-box binding protein 1, short), which is also associated with ER stress, were significantly upregulated in mutant mice (Figure 3A through 3C). To determine whether the ERAD pathway might be involved in the degradation of CASQ2 and TRDN, isolated neonatal cardiomyocytes were treated for 8 hours with the ERAD pathway inhibitor eeyarestatin. The results showed an increase in CASQ2 protein levels in *Casq2*$^{R33Q/R33Q}$ neonatal cardiomyocytes treated with eeyarestatin, compared with untreated *Casq2*$^{R33Q/R33Q}$ neonatal cardiomyocytes, whereas TRDN levels remained unchanged (Figure 3D and 3E). These results pointed toward distinct degradation pathways for the different couplon proteins.

CASQ2 But Not TRDN Is Degraded by the Ubiquitin-Proteasome System

Given the increase in proteasome-related proteins identified in the proteomics analysis, we explored whether the ubiquitin-proteasome system (UPS) was involved in the degradation of couplon proteins in *Casq2*$^{R33Q/R33Q}$ mice. Neonatal cardiomyocytes isolated from *Casq2*$^{R33Q/R33Q}$ and *Casq2*$^{WT/WT}$ mice were treated with the proteasome inhibitor MG132 or vehicle. Results showed an increase in CASQ2 levels in *Casq2*$^{R33Q/R33Q}$ treated cardiomyocytes compared with untreated cells, whereas TRDN remained unchanged (Figure 4A and 4B). To confirm these changes in vivo, *Casq2*$^{R33Q/R33Q}$ and WT adult mice were injected intraperitoneally with the proteasome inhibitor bortezomib or vehicle once a day for 3 consecutive days. CASQ2 protein levels were increased in bortezomib-treated *Casq2*$^{R33Q/R33Q}$ mice, while no changes were observed in TRDN or JCTN protein levels (Figure 4C and 4D), confirming the results obtained in neonatal cardiomyocytes. These results suggested that the UPS is necessary for CASQ2 degradation in CPVT.

CASQ2 Is Partially Degraded Through Autophagy in *Casq2*$^{R33Q/R33Q}$ Mice

Previous studies have reported connections between the UPS and autophagy pathways. More specifically, when the ER stress response and the ERAD system are insufficient to restore ER homeostasis, additional degradation pathways are activated, including autophagy.[20,21] To determine whether autophagy was altered in this CPVT model, we first looked for changes in the global autophagic flux by measuring the amount of LC3II protein in neonatal cardiomyocytes from mutant and WT mice by Western blot. After treatment with the autophagosome-lysosome fusion inhibitor hydroxychloroquine, LC3II protein levels were significantly increased in cardiomyocytes from *Casq2*$^{R33Q/R33Q}$ compared with those of *Casq2*$^{WT/WT}$ mice (Figure 5A and 5B), suggesting increased autophagic flux. In addition, we found an increase in LAMP1 in protein extracts from *Casq2*$^{R33Q/R33Q}$ mice (Figure 5C and 5D).

Interestingly, we found that CASQ2 protein levels increased when neonatal cardiomyocytes isolated from *Casq2*$^{R33Q/R33Q}$ mice were treated with hydroxychloroquine compared with those of untreated *Casq2*$^{R33Q/R33Q}$ mice, whereas there were no changes in TRDN protein levels (Figure 5E and 5F). To validate these changes in vivo, *Casq2*$^{R33Q/R33Q}$ and *Casq2*$^{WT/WT}$ mice were treated with chloroquine for 24 hours, and protein extracts were analyzed using Western blot. Autophagy flux inhibition with chloroquine prevented CASQ2 degradation in *Casq2*$^{R33Q/R33Q}$ mouse hearts, whereas TRDN and JCTN remained unchanged (Figure 5G and 5H), suggesting that autophagy partially mediates CASQ2 degradation. No changes in protein levels were observed when WT mice were treated with chloroquine.

Calpain Is Activated in *Casq2*$^{R33Q/R33Q}$ Mice and Mediates Couplon Protein Degradation

Alterations in calcium homeostasis and ER stress may activate calcium-dependent proteolytic enzymes, such as calpain.[22–25] Therefore, we hypothesized that calpain could play an important role in the degradation of

Downloaded from http://ahajournals.org by on November 5, 2026

Downloaded from http://ahajournals.org by on November 5, 2026

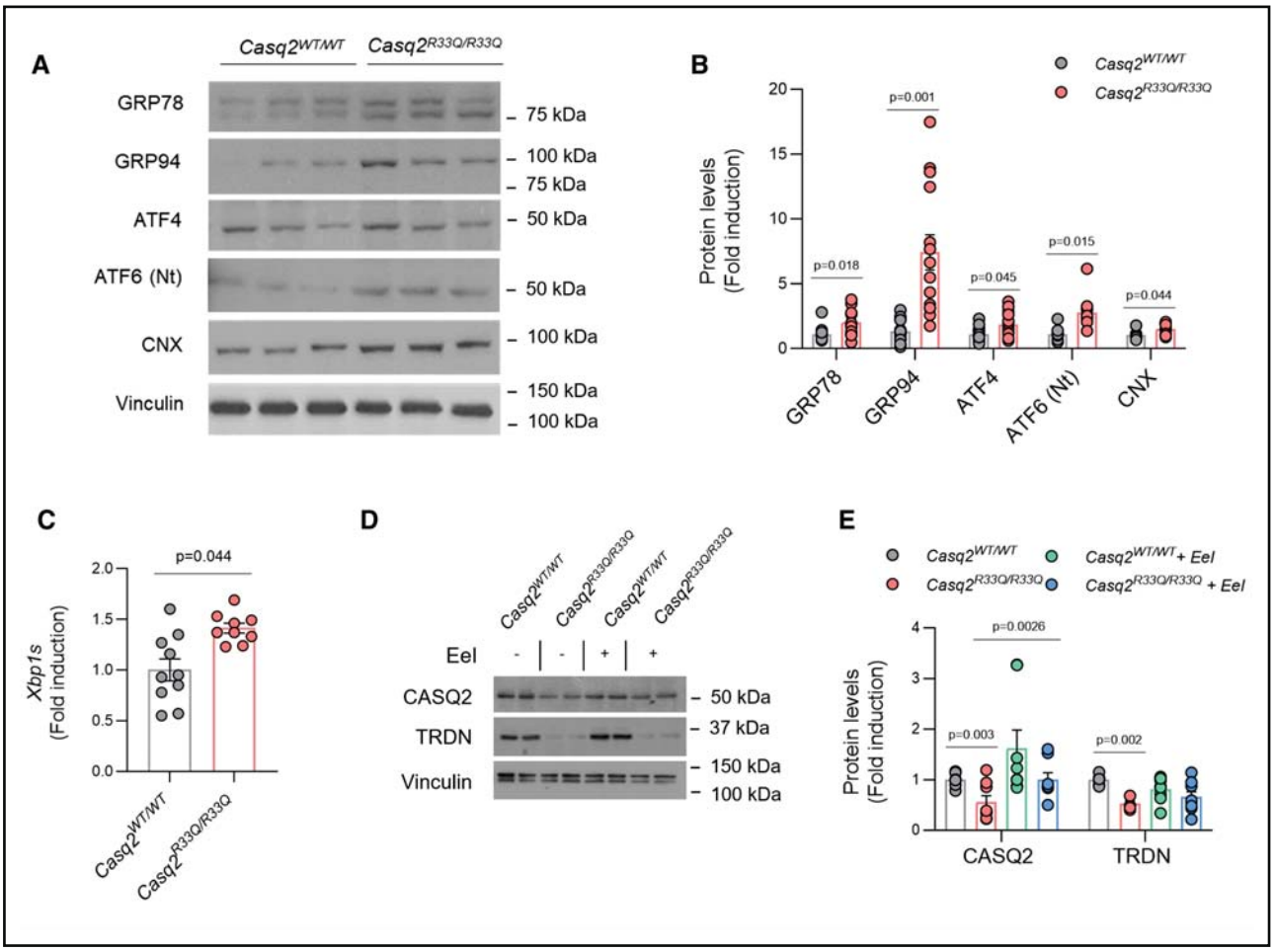


Figure 3. Endoplasmic reticulum (ER) stress and the unfolded protein response are activated in *Casq2*$^{R33Q/R33Q}$ mice and mediate CASQ2 (calsequestrin 2) degradation.

A and **B**, Markers of ER stress and unfolded protein response (UPR) were assessed by Western blot, and the band intensities were quantified. Vinculin was used as a loading control. n=15 (GRP78), 13 (GRP94), 14 (ATF4), 9 (ATF6), and 8 (CNX) mice per group. **C**, XBP1s (X-box binding protein 1, short) mRNA levels were analyzed by quantitative reverse-transcribed (qRT)-polymerase chain reaction. Data are represented as fold change over the values of *Casq2*$^{WT/WT}$ mice. **B** and **C**, Mutiple *t* tests with adjusted *P* value (**B**) or Mann-Whitney *U* test (**C**) were used. n=9 (wild-type) and 10 (mutant) mice per group. **D** and **E**, Protein extracts from *Casq2*$^{R33Q/R33Q}$ and *Casq2*$^{WT/WT}$ neonatal cardiomyocytes treated or untreated with the endoplasmic reticulum–associated degradation (ERAD) pathway inhibitor eeyarestatin (Eel) were analyzed by Western blot and quantified. Data are represented as fold induction±SEM over the values of untreated *Casq2*$^{WT/WT}$ neonatal cardiomyocytes. Two-way ANOVA followed by a Dunnett multiple comparison test was used. n=8 per group. ATF4 indicates activating transcription factor 4; ATF6, activating transcription factor 6; CNX, Ca^{2+}-binding protein calnexin; Eel, eeyarestatin I; GRP78, glucose-regulated protein 78; GRP94, glucose-regulated protein 94; and TRDN, triadin.

couplon proteins. Western blot analysis showed a significant increase in CAPN1 (calpain 1) protein levels in *Casq2*$^{R33Q/R33Q}$ mice and a decrease in the endogenous calpain inhibitor CAST, which regulates the activity of CAPN1 and CAPN2 (Figure 6A and 6B). In addition, *Casq2*$^{R33Q/R33Q}$ mice showed a significant increase in the cleavage of α-fodrin (alpha-fodrin), a known calpain target that often serves as an indicator of calpain activity. A strong increase was observed in the cleaved (150 kDa) to full-length (240 kDa) α-fodrin ratio (Figure 6C and 6D), suggesting that calpain activity was increased in *Casq2*$^{R33Q/R33Q}$ mice. To determine whether calpain inhibition could prevent couplon protein degradation, neonatal cardiomyocytes from *Casq2*$^{R33Q/R33Q}$ and *Casq2*$^{WT/WT}$ mice were treated with calpeptin for 8 hours. An increase in CASQ2 and TRDN levels was detected in *Casq2*$^{R33Q/R33Q}$ neonatal cardiomyocytes treated with calpeptin compared with untreated controls (Figure 7A and 7B). To confirm these results in vivo, *Casq2*$^{R33Q/R33Q}$ mice were injected intraperitoneally with the calpain inhibitor MDL28170 for 3 days. Western blot analysis of myocardial samples showed a decrease in α-fodrin cleavage in the treated mice, indicating that the inhibitor was effective (Figure 7C and 7D). Importantly, a significant increase in CASQ2 and TRDN protein levels was observed after calpain inhibition, accompanied by increased JCTN protein levels (Figure 7E and 7F). Furthermore, restoration of TRDN and CASQ2 expression significantly reduced

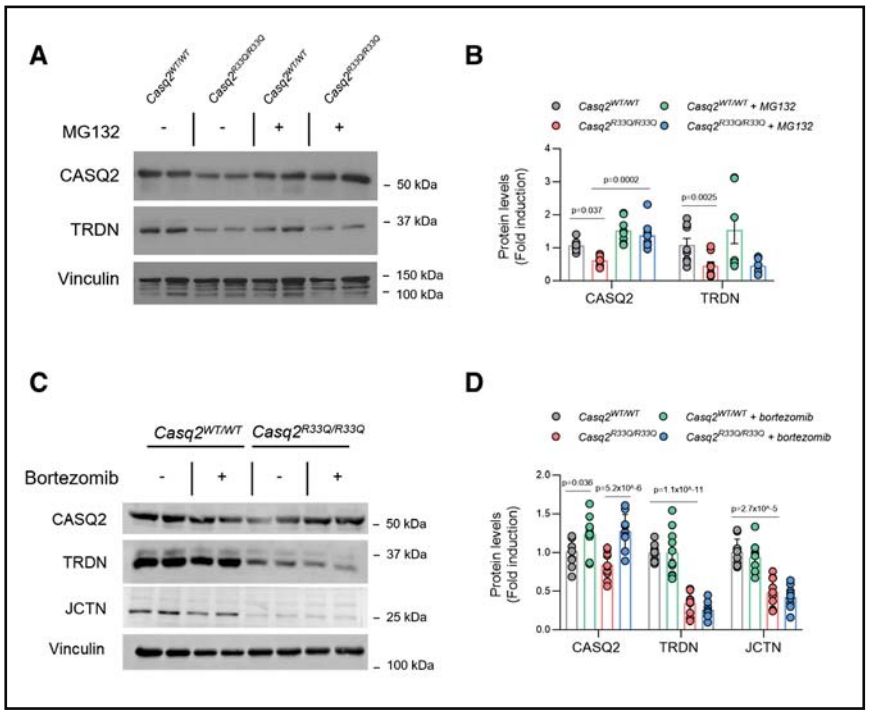


Figure 4. CASQ2 (calsequestrin 2) is degraded by the proteasome in *Casq2*$^{R33Q/R33Q}$ mice.
A and **B**, Protein levels extracted from Casq2R33Q/R33Q and Casq2WT/W^{T} neonatal cardiomyocytes treated or untreated with the proteasome inhibitor MG132 were analyzed by Western blot and quantified. Vinculin loading control is shown. Data are represented as fold induction±SEM over the values of untreated *Casq2*$^{WT/WT}$ neonatal cardiomyocytes. Two-way ANOVA with Tukey multiple comparison test was used. n=8 per group. **C** and **D**, CASQ2, TRDN (triadin), and JCTN (junctin) protein levels from *Casq2*$^{R33Q/R33Q}$ and *Casq2*$^{WT/WT}$ mice treated or untreated with the proteasome inhibitor bortezomib were analyzed by Western blot and quantified. Data are represented as fold induction±SEM over the values of untreated *Casq2*$^{WT/WT}$ mice. Two-way ANOVA with Tukey multiple comparison test was used. n=10 per group.

the levels of ER stress–related proteins GRP78 and GRP94 (Figure 7G and 7H). To confirm the increase in TRDN and CASQ2 expression after calpain inhibition, we treated *Casq2*$^{R33Q/R33Q}$ mice with a second calpain inhibitor in vivo. As shown in Figure S3A and S3B, calpeptin treatment resulted in a significant upregulation of TRDN and CASQ2, confirming the results obtained with MDL28170.

Finally, we explored whether TRDN could be a direct calpain substrate. Incubation of recombinant human TRDN with recombinant calpain in vitro resulted in strong cleavage of TRDN that was prevented by the calpain inhibitor calpeptin (Figure S4A and S4B). Similarly, recombinant calpain cleaved mouse TRDN in extracts from WT neonatal cardiomyocytes, and this processing was inhibited by calpeptin (Figure S4C and S4D). These results demonstrate that TRDN is a direct target of calpain, supporting the hypothesis that increased calpain activity contributes to couplon protein degradation in *Casq2*$^{R33Q/R33Q}$ hearts.

Calpain Inhibition Improves the VT Phenotype in *Casq2*$^{R33Q/R33Q}$ Mice

To investigate whether the increase in calpain activity could play a detrimental role in the development of CPVT, we first investigated whether calpain inhibition improved calcium handling in adult mutant mice. Cardiomyocytes isolated from adult *Casq2*$^{R33Q/R33Q}$ mice showed a significantly higher propensity for developing triggered activity as compared with WT counterparts, particularly when exposed to isoproterenol, in line with our previous results with these mice[26] (Figure 8A through 8C). Mutant mice treated with flecainide were significantly less likely to develop triggered activity, as expected (Figure 8A through 8C; Table S3). Importantly, exposure of adult *Casq2*$^{R33Q/R33Q}$ mice to the calpain inhibitor MDL28170 also reduced triggered activity (odds ratio, 0.2 [95% CI, 0.1–0.6]; Figure 8A through 8C; Table S3). Because flecainide and MDL28170 were administered to the animals before cardiomyocyte isolation and were absent during Ca^{2+} imaging, these findings indicate that the reduction in triggered activity persisted after drug removal, consistent with changes induced in vivo rather than an acute effect of the compounds during Ca^{2+} recording.

In our calcium imaging recordings, triggered events were consistently preceded by spontaneous diastolic Ca^{2+} waves. These spontaneous Ca^{2+} release events displayed a consistent latency measured from the prior diastole and were visually identifiable as discrete propagating mini-waves. We did not observe biphasic or dome-and-plateau Ca^{2+} release patterns, nor the irregular Ca^{2+} dynamics typically associated with early afterdepolarizations. Instead, the observed patterns are more consistent with delayed afterdepolarization–mediated triggered activity.

To determine whether this improvement translated into arrhythmia susceptibility, an ECG telemetry device was implanted into *Casq2*$^{R33Q/R33Q}$ mice. As shown in Figure 8D and 8E, treatment with the calpain inhibitor MDL28170 for 3 days significantly reduced the incidence of ventricular arrhythmias after adrenergic stimulation (epinephrine, 2 mg/kg), indicating that calpain inhibition improves both cellular Ca^{2+} handling and susceptibility to ventricular arrhythmias in *Casq2*$^{R33Q/R33Q}$ mice.

Downloaded from http://ahajournals.org by on November 5, 2026

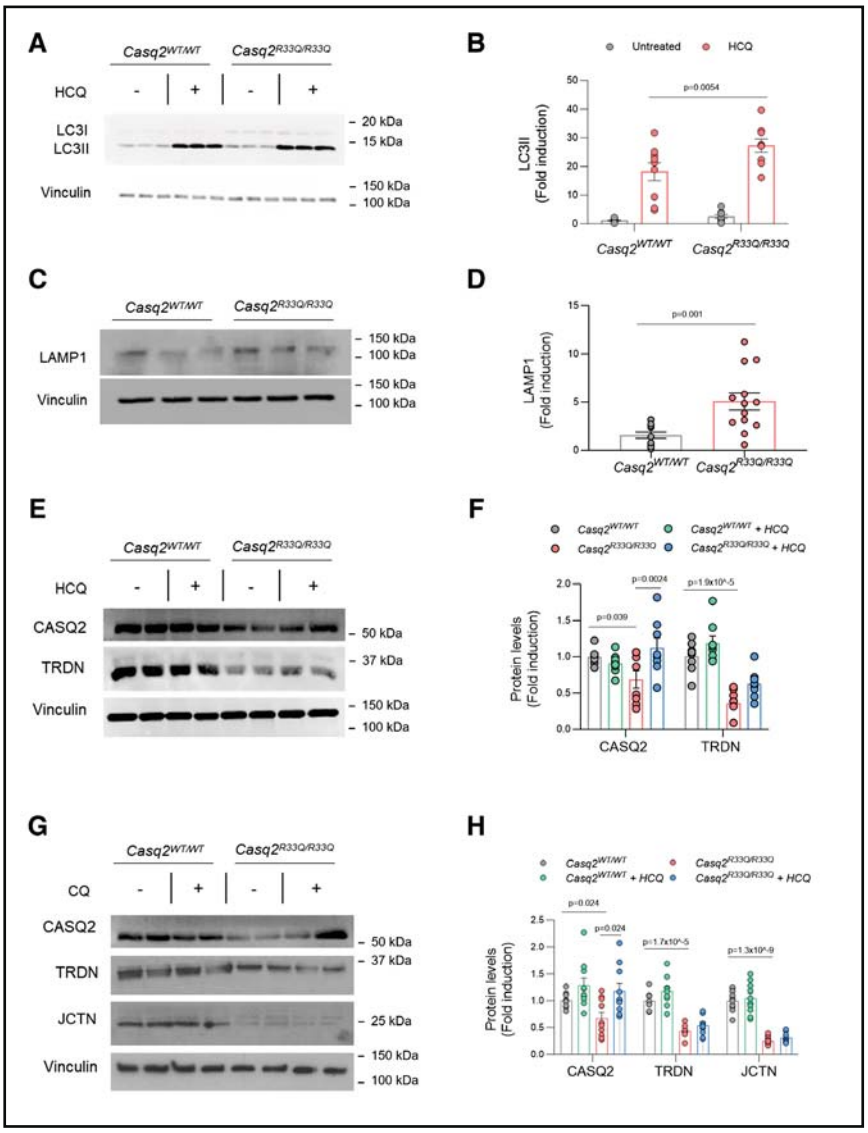


Figure 5. *Casq2*$^{R33Q/R33Q}$ mice showed an altered autophagic flux leading to CASQ2 (calsequestrin 2) degradation.
A and **B**, LC3II protein levels were analyzed by Western blot in *Casq2*$^{WT/WT}$ and *Casq2*$^{R33Q/R33Q}$ neonatal cardiomyocytes treated or untreated with hydroxychloroquine (HCQ), and the band intensity was quantified. Vinculin was used as a loading control. **C** and **D**, LAMP1 (lysosome-associated membrane glycoprotein 1) expression was analyzed by Western blot (**C**) in myocardial samples from *Casq2*$^{WT/WT}$ and *Casq2*$^{R33Q/R33Q}$ mice and quantified (**D**). **B** and **D**, Data are represented as fold induction±SEM over the values of untreated *Casq2*$^{WT/WT}$ neonatal cardiomyocytes or mice. Šídák multiple comparisons test (**B**) or Mann-Whitney *U* test (**D**) was used. n=9 (**B**) or n=13 (**D**) per group. **E** and **F**, CASQ2 and TRDN (triadin) levels were analyzed by Western blot in *Casq2*$^{R33Q/R33Q}$ and *Casq2*$^{WT/WT}$ neonatal cardiomyocytes treated or untreated with HCQ (**E**), and band intensity was quantified (**F**). Vinculin loading control is shown. Data are represented as fold induction±SEM over the values of *Casq2*$^{WT/WT}$ neonatal cardiomyocytes. Two-way ANOVA with Dunnett multiple comparison test was used. n=8 per group. **G** and **H**, Couplon protein levels were analyzed by Western blot in myocardial samples from *Casq2*$^{R33Q/R33Q}$ and *Casq2*$^{WT/WT}$ mice treated or untreated with chloroquine (CQ). Data are represented as fold induction±SEM over the values of untreated *Casq2*$^{WT/WT}$ mice. Two-way ANOVA with Tukey multiple comparison test was used. n=10 per group. CQ indicates chloroquine; HCQ, hydroxychloroquine; and LAMP1, lysosome-associated membrane glycoprotein 1.

DISCUSSION

CPVT is caused by mutations mainly in couplon proteins that compromise effective Ca^{2+} handling in cardiomyocytes. The recessive form of the disease caused by the R33Q mutation in CASQ2 is characterized by degradation of CASQ2 itself and the proteins that link it to RyR2 in the SR membrane. In this work, we shed light on the mechanisms underlying couplon protein degradation, and we demonstrate that calpain-dependent proteolysis contributes to the development of the disease phenotype.

The proteomics analysis unveiled 2 novel mechanisms contributing to SR Ca^{2+} mishandling in CASQ2 mutant mice. On the one hand, the increased SR Ca^{2+} leak through RyR2 during diastole in *Casq2*$^{R33Q/R33Q}$ mice could be exacerbated by higher levels of HRC, an SR Ca^{2+} binding protein that regulates SR Ca^{2+} by interacting

Downloaded from http://ahajournals.org by on November 5, 2026

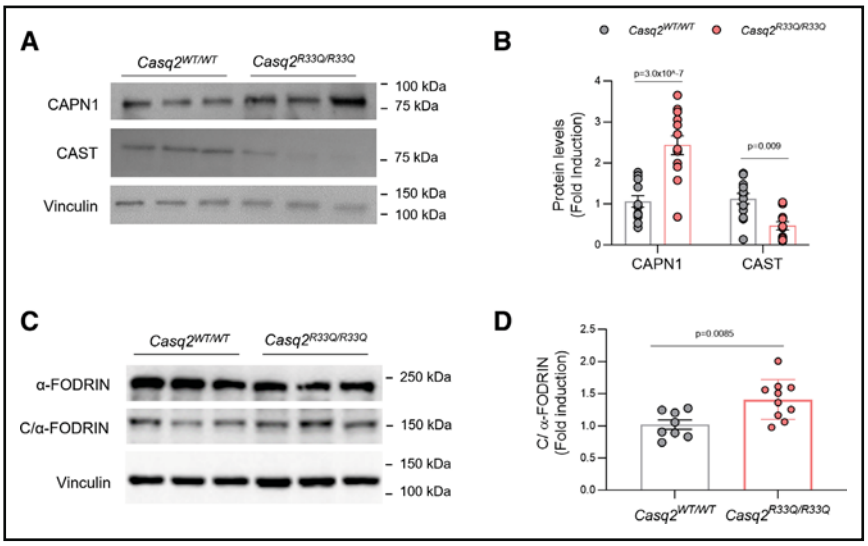


Figure 6. Calpain activity is increased in *Casq2*$^{R33Q/R33Q}$ mice.
A and **B**, Expression of CAPN1 (calpain 1) and CAST proteins in myocardial samples from Casq2R33Q/R33Q and Casq2WT/WT mice was analyzed by Western blot (**A**), and the band intensity was quantified (**B**). Vinculin was used as a loading control. **C**, The degree of calpain activation was determined by analyzing cleavage of the calpain target α-fodrin (alpha-fodrin) by Western blot in myocardial samples from *Casq2*$^{R33Q/R33Q}$ and *Casq2*$^{WT/WT}$ mice. **D**, The intensity of Western blot bands was quantified and expressed as the α-fodrin 150/240 kDa ratio. Data are represented as fold induction±SEM over the values of *Casq2*$^{WT/WT}$ mice. **B** and **D**, Data are expressed as fold induction±SEM over the values of *Casq2*$^{WT/WT}$ mice; 2-way ANOVA with Šídák's multiple comparisons test (**B**) and Mann-Whitney *U* test (**D**) were used. n=13 (**B**) and n=8 to 10 (**D**). C/α-fodrin indicates processed α-fodrin; CAPN1, calpain 1; CASQ2, calsequestrin 2; CAST, calpastatin; JCTN, junctin; and TRDN, triadin.

Downloaded from http://ahajournals.org by on November 5, 2026

with SERCA2a and TRDN.[27–29] In addition, HRC showed increased phosphorylation at Ser96, which strengthens its interaction with TRDN.[30] Both HRC and CASQ2 compete for TRDN binding with opposite effects on RyR2 activity.[29] Our findings suggest that in *Casq2*$^{R33Q/R33Q}$ mice, the lack of Ca^{2+} buffering by CASQ2 combined with the increase in HRC expression and phosphorylation could result in increased Ca^{2+} leak through the RyR2 during diastole. On the other hand, SERCA2a inhibition resulting from decreased P-PLN at Ser16 and Thr17 would limit SR Ca^{2+} uptake, thereby reducing the SR Ca^{2+} content. Interestingly, inhibition of RyR2 Ca^{2+} leak with flecainide, which has proven successful for the treatment of patients with CPVT,[17] partially restored couplon protein levels, suggesting that CASQ2 and TRDN degradation was a consequence rather than a cause of SR Ca^{2+} leakage, at least partially.

We therefore explored proteolysis mechanisms that could be activated by alterations in calcium homeostasis and could be responsible for the degradation of these proteins. It is well known that changes in Ca^{2+} concentration trigger ER stress signaling to restore ER homeostasis.[31] In this study, we confirmed the increase in ER stress markers GRP78 and GRP94 previously reported in *Casq2*$^{R33Q/R33Q}$ mice[31] and identified an increase in additional unfolded protein response components, including ATF4, ATF6, CNX, and *Xbp1s*. The unfolded protein response restores ER homeostasis by promoting protein degradation through the ERAD pathway,[32] which targets ER proteins for ubiquitination[33] and retrotranslocates them out of the ER for further degradation by the UPS and by the lysosome as part of autophagy.[34–36] CASQ2 levels were restored after inhibition of the ERAD pathway, suggesting an active role of ER stress in the degradation of this protein in *Casq2*$^{R33Q/R33Q}$ mice. Concomitant with ER stress, we observed increased autophagic flux in mutant mice. In addition, CASQ2 levels were partially restored when either the proteasome or autophagy was inhibited, both in vitro and in vivo, clearly delineating the pathways followed by CASQ2 R33Q for its degradation. Interestingly, TRDN and JCTN levels remained unchanged in the presence of ERAD, proteasome, or autophagy inhibitors, suggesting that couplon proteins are degraded through different mechanisms.

In addition to activation of the ER stress response, *Casq2*$^{R33Q/R33Q}$ mice showed increased expression and activity of calpain, a protease activated by Ca^{2+} that plays a role in cardiac homeostasis and in different myocardial pathologies.[37–40] Calpain inhibition improves cardiac function and reduces infarct expansion in rodent models of myocardial infarction,[41,42] and recent work in a RyR2-S2236L CPVT model also supports a role for calpain-dependent mechanisms in arrhythmogenesis through mitochondrial OPA1 (OPA1 mitochondrial dynamin like GTPase) cleavage.[43] Here, we identify TRDN as a direct calpain target and show that calpain inhibition increased CASQ2, TRDN, and JCTN protein levels in CASQ2 mutant mice, unveiling a key role for this protease in couplon protein degradation in

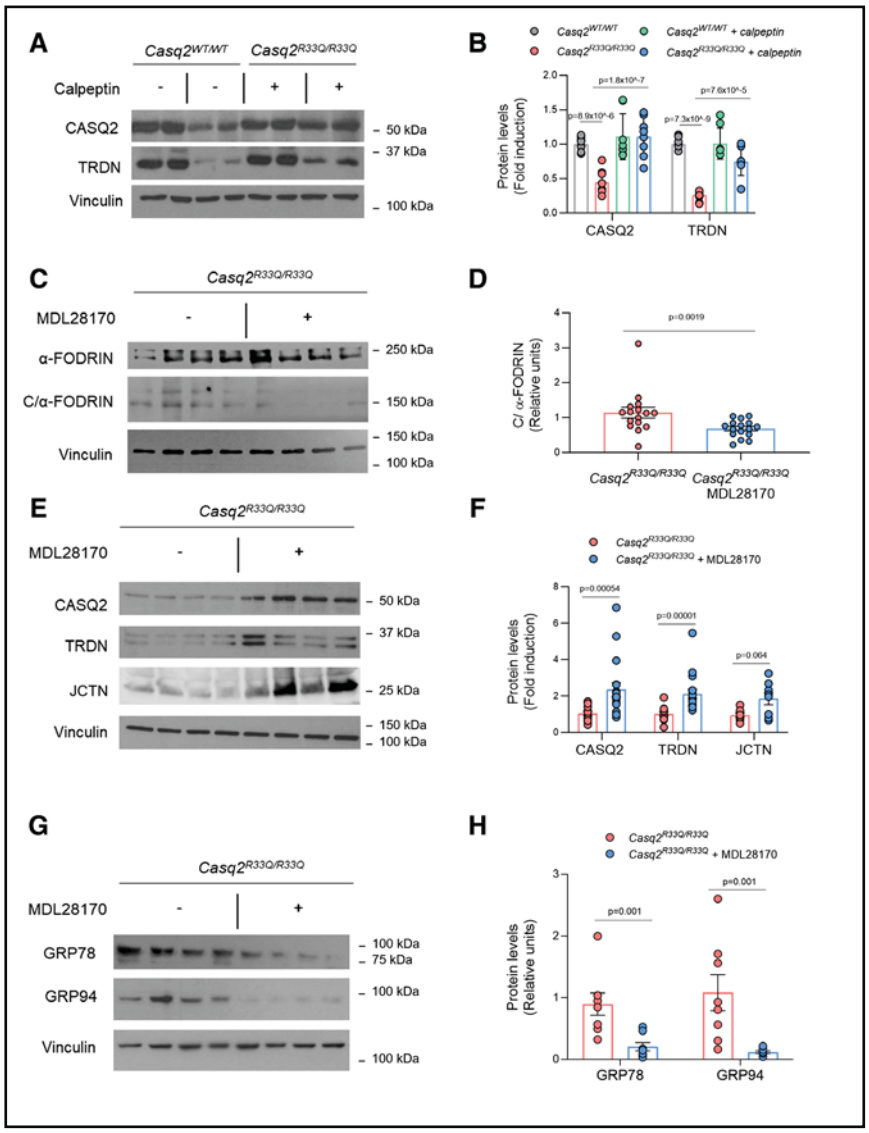


Figure 7. CASQ2 (calsequestrin 2), TRDN (triadin), and JCTN (junctin) protein levels are increased after calpain inhibition.
A and **B**, Proteins extracted from *Casq2*$^{WT/WT}$ and *Casq2*$^{R33Q/R33Q}$ neonatal cardiomyocytes treated or untreated with the calpain inhibitor calpeptin at 10 µM for 8 hours were analyzed by Western blot (**A**) and quantified (**B**). Vinculin was used as a loading control. Data are represented as fold induction±SEM over the values of *Casq2*$^{WT/WT}$ untreated neonatal cardiomyocytes. Two-way ANOVA with Tukey multiple comparison test. n=8 per group. **C** through **F**, Proteins extracted from *Casq2*$^{R33Q/R33Q}$ mice treated or untreated with the calpain inhibitor MDL28170 at 70 mg/kg, administered once daily for 3 days, were analyzed by Western blot (**C** and **E**), and the band intensity was quantified (**D** and **F**). Data are represented as fold induction±SEM over the values of untreated *Casq2*$^{R33Q/R33Q}$ mice. Mann-Whitney *U* test was used; n=16 per group (**D**). Multiple nonparametric *t* tests with adjusted *P* values were used, n=8 (JCTN) to 13 (CASQ2, TRDN) per group (**F**). **G** and **H**, Western blot of the ER stress–related markers GRP78 (glucose-regulated protein 78) and GRP94 from myocardium of *Casq2*$^{R33Q/R33Q}$ mice treated or untreated with MDL28170. Vinculin loading control is shown. Data are represented as fold induction±SEM over the values of untreated *Casq2*$^{R33Q/R33Q}$ mice. Multiple nonparametric *t* tests with adjusted *P* values were used. n=8 per group. CASQ2 indicates calsequestrin 2; GRP78 and 94, glucose-regulated protein 78 and 94; JCTN, junctin; and TRDN, triadin.

CPVT. Calpain inhibition was the only treatment that increased TRDN and JCTN protein levels in *Casq2*$^{R33Q/R33Q}$ mice, in addition to CASQ2. Most importantly, the increase in the levels of the couplon proteins was accompanied by an improvement of the pathological phenotype, as reflected by an improvement in calcium handling and a decrease in VT episodes in *Casq2*$^{R33Q/R33Q}$ mice treated with the calpain inhibitor. Notably, the improvement in calcium handling persisted in cardiomyocytes isolated from treated animals and studied in the absence of the inhibitor, consistent with a sustained effect of calpain inhibition on the cellular phenotype. To our knowledge, this is the first description of the involvement of calpain in CPVT in vivo, suggesting that calpain may be a potential therapeutic target for this disease.

In addition to the identification of distinct mechanisms, our results suggest an unexpected change in the order of events leading to couplon protein degradation. We found that in the presence of mutant CASQ2, TRDN is degraded faster than CASQ2-R33Q. Furthermore, CASQ2-R33Q expression is recovered when TRDN levels are restored, both through overexpression and through calpain inhibition, whereas prevention of CASQ2 degradation has no impact on TRDN stability. These results suggest that TRDN degradation precedes and contributes to CASQ2-R33Q destabilization rather than occurring as a consequence of CASQ2 degradation. Together, our results support a model in which SR Ca^{2+} leakage leads to calpain activation and TRDN degradation, thereby promoting subsequent CASQ2 degradation.

In conclusion, our study highlights the important role of proteostasis in CPVT. It shows how specific protein degradation pathways target the different couplon proteins and unveils an unexpected order of events. Importantly, calpain proteolytic activity was identified as a potential therapeutic target for CPVT, either alone or in

Downloaded from http://ahajournals.org by on November 5, 2026

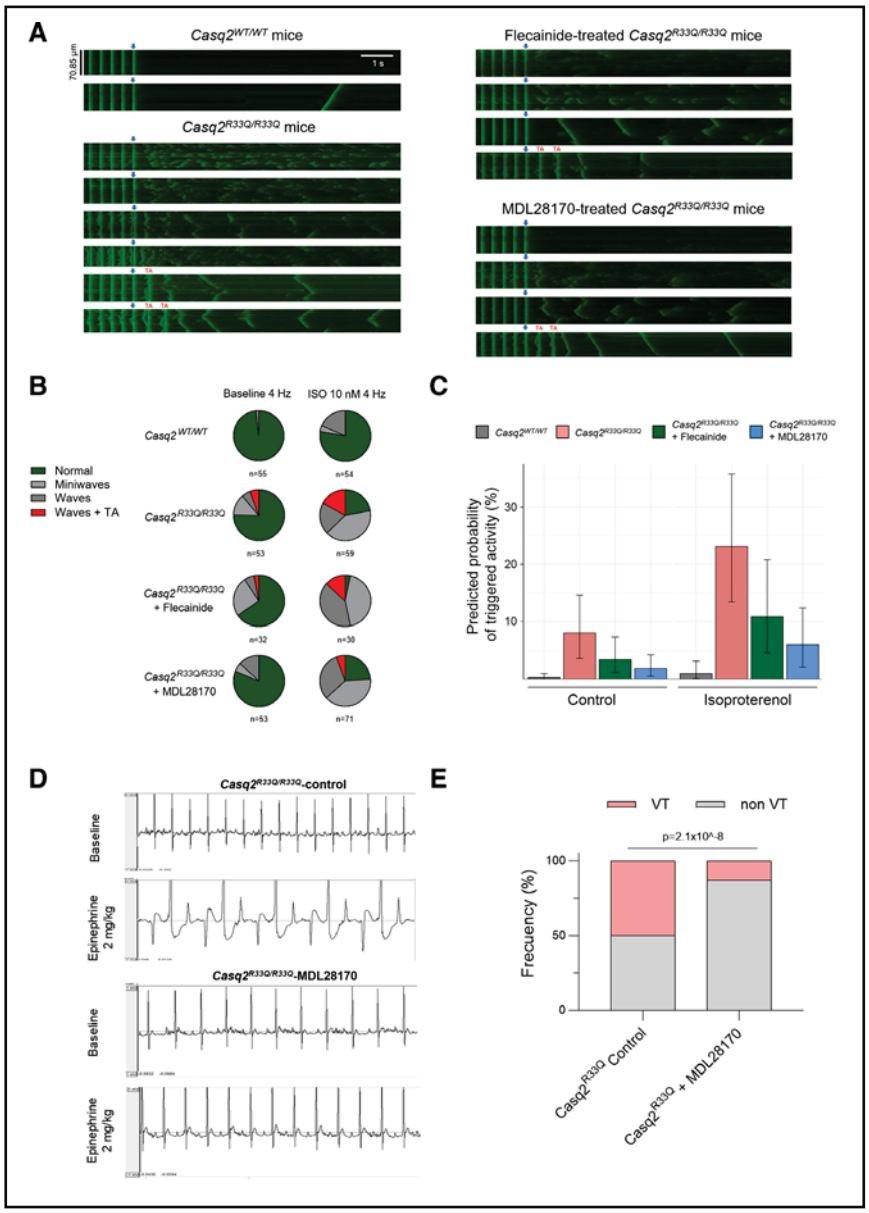


Figure 8. Calpain inhibition improves the pathological phenotype of *Casq2*$^{R33Q/R33Q}$ mice.
Adult Casq2WT/WT or Casq2R33Q/R33Q mice were treated with 20 µmol/L flecainide or 70 mg/kg MDL28170 for 3 days, where indicated, and ventricular cardiomyocytes were isolated. Ca^{2+} imaging was performed in field-stimulated Fluo-4 AM-loaded cells in compound-free Tyrode solution at physiological temperature. Note that animals, not cells, were treated with either flecainide or MDL 28170. **A,** Raw line-scan images showing examples of the observed phenotypes in isolated ventricular myocytes from each experimental group. **B**, Pie chart displaying a quantification on a per-cell basis of the phenotypic spectrum found. **C**, Data were analyzed hierarchically (ie, per animal and per cell basis) using a Bayesian logistic regression to model the probability of triggered activity, using *Casq2*$^{R33Q/R33Q}$ as reference. **D**, *Casq2*$^{R33Q/R33Q}$ mice were treated with 70 mg/kg per day MDL28170 for 3 days, and ECGs were recorded 15 minutes after administration of epinephrine. ECGs recorded at baseline and after epinephrine administration are shown. **E**, Percentage of *Casq2*$^{R33Q/R33Q}$ mice with incidence of sustained ventricular tachycardia (VT) after epinephrine administration in animals treated or untreated with MDL28170. Data were analyzed using contingency tables with the Fisher exact test. n=8 mice per group. CASQ2 indicates calsequestrin 2; ISO, isoproterenol; JCTN, junctin; TA, triggered activity; TRDN, triadin; and VT, ventricular tachycardia.

Downloaded from http://ahajournals.org by on November 5, 2026

combination, paving the way for the development of new treatments for this disease.

We acknowledge the following limitations of our study: although we observed an increase in the concentration of TRDN and CASQ2 in mutant mice treated with flecainide, we cannot rule out that the effect of this treatment was due to a mechanism unrelated to calcium handling. It remains to be investigated whether TRDN degradation by calpain is also operational in other forms of CPVT or other cardiac diseases, which would broaden the impact of our findings. Additional animal models and controls are necessary before translating these findings to the clinical setting. Finally, it should be noted that while treatments that limit protein degradation may be effective for some proteins, these treatments might have a detrimental effect on the processing and degradation of other proteins that need to be removed from the cell.

ARTICLE INFORMATION

Received May 07, 2026; revision received August 13, 2026; accepted September 4, 2026.

Affiliations

Centro Nacional de Investigaciones Cardiovasculares (CNIC), Madrid, Spain (L.R.-H., D.J.S., R.F.S.-B., A.C., L.E.-M., E.C., M.L.-O., A.G.-C., J.M.V., M.T., S.G.P., E.L.-P.). Centro de Investigación Biomédica en Red Cardiovascular (CIBERCV), Madrid, Spain (E.C., J.M.V., M.T., E.L.-P.). Department of Molecular Medicine, University of Pavia, Italy (D.K., S.G.P.). Molecular Cardiology Unit, IRCCS Istituti Clinici Scientifici Maugeri, Pavia, Italy (D.K., S.G.P.).

Acknowledgments

We thank the Center for Cardiovascular Research (CNIC) animal facility for mouse breeding, the Viral Vectors Unit for adeno-associated virus (AAV) production, and the Proteomics Unit for analyses.

Sources of Funding

This project was funded by the Pathfinder Cardiogenomics program of the European Innovation Council of the European Union (DCM-NEXT project; project number 101115416) to E. Lara-Pezzi, and by grant PID2024-155919OB-I00,

funded by the Ministerio de Ciencia, Innovación y Universidades, Spain (MCIN/AEI/10.13039/501100011033), by the European Union's NextGenerationEU/PRTR (Plan de Recuperación, Transformación y Resiliencia de España) and by FEDER, to E. Lara-Pezzi. The work was also supported by grants from the European Research Council (ERC; grant agreement 101142005) and Comunidad de Madrid (P2022/BMD-7245 CARDIOBOOST-CM) to M. Torres. The Center for Cardiovascular Research (CNIC) is supported by the Instituto de Salud Carlos III (ISCIII), the Ministerio de Ciencia, Innovación y Universidades (MICIU), and the Pro CNIC Foundation, and is a Severo Ochoa Center of Excellence (grant CEX2025-001658-S, funded by MICIU AEI/10.13039/501100011033).

Disclosures

None.

Supplemental Material

Supplemental Methods
Tables S1–S3
Figures S1–S4
Major Resources Table
Uncropped Western Blots
Data Set
ARRIVE Guidelines
References 12,18,44–52

Downloaded from http://ahajournals.org by on November 5, 2026

REFERENCES

1. Wleklinski MJ, Kannankeril PJ, Knollmann BC. Molecular and tissue mechanisms of catecholaminergic polymorphic ventricular tachycardia. *J Physiol*. 2020;598:2817–2834. doi: 10.1113/JP276757
2. Napolitano C, Mazzanti A, Bloise R, Priori SG. Catecholaminergic polymorphic ventricular tachycardia. Electrocardiography of inherited arrhythmias and cardiomyopathies: from basic science to clinical practice. Gene Reviews. Accessed July 1, 2026. https://www.ncbi.nlm.nih.gov/books/NBK1289/
3. Priori SG, Mazzanti A, Santiago DJ, Kukavica D, Trancuccio A, Kovacic JC. Precision medicine in catecholaminergic polymorphic ventricular tachycardia: JACC Focus Seminar 5/5. *J Am Coll Cardiol*. 2021;77:2592–2612. doi: 10.1016/j.jacc.2020.12.073
4. Bezzina CR, Lahrouchi N, Priori SG. Genetics of sudden cardiac death. *Circ Res*. 2015;116:1919–1936. doi: 10.1161/CIRCRESAHA.116.304030
5. Li L, Mirza S, Richardson SJ, Gallant EM, Thekkedam C, Pace SM, Zorzato F, Liu D, Beard NA, Dulhunty AF. A new cytoplasmic interaction between junctin and ryanodine receptor Ca^{2+} release channels. *J Cell Sci*. 2015;128:951–963. doi: 10.1242/jcs.160689
6. Martínez-Bartolomé S, Navarro P, Martín-Maroto F, López-Ferrer D, Ramos-Fernández A, Villar M, García-Ruiz JP, Vázquez J. Properties of average score distributions of SEQUEST: the probability ratio method. *Mol Cell Proteomics*. 2008;7:1135–1145. doi: 10.1074/mcp.M700239-MCP200
7. Navarro P, Vazquez J. A refined method to calculate false discovery rates for peptide identification using decoy databases. *J Proteome Res*. 2009;8:1792–1796. doi: 10.1021/pr800362h
8. Schwartz PJ, Ackerman MJ, Antzelevitch C, Bezzina CR, Borggrefe M, Cuneo BF, Wilde AAM. Inherited cardiac arrhythmias. *Nat Rev Dis Primers*. 2020;6:58. doi: 10.1038/s41572-020-0188-7
9. Peltenburg PJ, Kallas D, Bos JM, Lieve KVV, Franciosi S, Roston TM, Denjoy I, Sorensen KB, Ohno S, Roses-Noguer F, et al. An international multicenter cohort study on β-blockers for the treatment of symptomatic children with catecholaminergic polymorphic ventricular tachycardia. *Circulation*. 2022;145:333–344. doi: 10.1161/CIRCULATIONAHA.121.056018
10. Roux-buisson N, Cacheux M, Fourest-lieuvin A, Fauconnier J, Brocard J, Denjoy I, Durand P, Guicheney P, Kyndt F, Leenhardt A, et al. Absence of triadin, a protein of the calcium release complex, is responsible for cardiac arrhythmia with sudden death in human. *Hum Mol Genet*. 2012;21:2759–2767. doi: 10.1093/hmg/dds104
11. Rizzi N, Liu N, Napolitano C, Nori A, Turcato F, Colombi B, Bicciato S, Arcelli D, Spedito A, Scelsi M, et al. Unexpected structural and functional consequences of the R33Q homozygous mutation in cardiac calsequestrin. *Circ Res*. 2008;103:298–306. doi: 10.1161/CIRCRESAHA.108.171660
12. Denegri M, Bongianino R, Lodola F, Boncompagni S, De Giusti VC, Avelino-Cruz JE, Liu N, Persampieri S, Curcio A, Esposito F, et al. Single delivery of an adeno-associated viral construct to transfer the CASQ2 gene to knock-in mice affected by catecholaminergic polymorphic ventricular tachycardia is able to cure the disease from birth to advanced age. *Circulation*. 2014;129:2673–2681. doi: 10.1161/CIRCULATIONAHA.113.006901
13. Leenhardt A, Lucet V, Denjoy I, Grau F, Ngoc DD, Coumel P. Catecholaminergic polymorphic ventricular tachycardia in children. *Circulation*. 1995;91:1512–1519. doi: 10.1161/01.cir.91.5.1512
14. Brand NJ, Lara-Pezzi E, Rosenthal N, Barton PJR. Analysis of cardiac myocyte biology in transgenic mice: a protocol for preparation of neonatal mouse cardiac myocyte cultures. *Methods Mol Biol*. 2010;633:113–124. doi: 10.1007/978-1-59745-019-5_9
15. Gustavsson M, Verardi R, Mullen DG, Mote KR, Traaseth NJ, Gopinath T, Veglia G. Allosteric regulation of SERCA by phosphorylation-mediated conformational shift of phospholamban. *Proc Natl Acad Sci USA*. 2013;110:17338–17343. doi: 10.1073/pnas.1303006110
16. Kryshtal DO, Blackwell DJ, Egly CL, Smith AN, Batiste SM, Johnston JN, Laver DR, Knollmann BC. RYR2 channel inhibition is the principal mechanism of flecainide action in CPVT. *Circ Res*. 2021;128:321–331. doi: 10.1161/CIRCRESAHA.120.316819
17. Bergeman AT, Lieve KVV, Kallas D, Bos JM, Noguer FR, Denjoy I, Zorio E, Kammeraad JAE, Peltenburg PJ, Tobert K, et al. Flecainide is associated with a lower incidence of arrhythmic events in a large cohort of patients with catecholaminergic polymorphic ventricular tachycardia. *Circulation*. 2023;148:2029–2037. doi: 10.1161/CIRCULATIONAHA.123.064786
18. Watanabe H, Chopra N, Laver D, Hwang HS, Davies SS, Roach DE, Duff HJ, Roden DM, Wilde AAM, Knollmann BC. Flecainide prevents catecholaminergic polymorphic ventricular tachycardia in mice and humans. *Nat Med*. 2009;15:380–383. doi: 10.1038/nm.1942
19. Liu N, Denegri M, Ruan Y, Avelino-Cruz JE, Perissi A, Negri S, Napolitano C, Coetzee WA, Boyden PA, Priori SG. Short communication: flecainide exerts an antiarrhythmic effect in a mouse model of catecholaminergic polymorphic ventricular tachycardia by increasing the threshold for triggered activity. *Circ Res*. 2011;109:291–295. doi: 10.1161/CIRCRESAHA.111.247338
20. Yorimitsu T, Nair U, Yang Z, Klionsky DJ. Endoplasmic reticulum stress triggers autophagy. *J Biol Chem*. 2006;281:30299–30304. doi: 10.1074/jbc.M607007200
21. Kwon J, Kim J, Kim KI. Crosstalk between endoplasmic reticulum stress response and autophagy in human diseases. *Anim Cells Syst*. 2023;27:29–37. doi: 10.1080/19768354.2023.2181217
22. Inserte J, Barba I, Hernando V, Garcia-Dorado D. Delayed recovery of intracellular acidosis during reperfusion prevents calpain activation and determines protection in postconditioned myocardium. *Cardiovasc Res*. 2009;81:116–122. doi: 10.1093/cvr/cvn260
23. Zatz M, Starling A. Calpains and disease. *N Engl J Med*. 2005;352:2413–2423. doi: 10.1056/NEJMra043361
24. Goll DE, Thompson VF, Li H, Wei W, Cong J. The calpain system. *Physiol Rev*. 2003;83:731–801. doi: 10.1152/physrev.00029.2002
25. Li S, Ma J, Li JB, Lacefield JC, Jones DL, Peng TQ, Wei M. Over-expression of calpastatin attenuates myocardial injury following myocardial infarction by inhibiting endoplasmic reticulum stress. *J Thorac Dis*. 2018;10:5283–5297. doi: 10.21037/jtd.2018.08.133
26. Liu N, Denegri M, Dun W, Boncompagni S, Lodola F, Protasi F, Napolitano C, Boyden PA, Priori SG. Abnormal propagation of calcium waves and ultrastructural remodeling in recessive catecholaminergic polymorphic ventricular tachycardia. *Circ Res*. 2013;113:142–152. doi: 10.1161/CIRCRESAHA.113.301783
27. Arvanitis DA, Vafiadaki E, Fan GC, Mitton BA, Gregory KN, Del Monte F, Kontrogianni-Konstantopoulos A, Sanoudou D, Kranias EG. Histidine-rich Ca-binding protein interacts with sarcoplasmic reticulum Ca-ATPase. *Am J Physiol Heart Circ Physiol*. 2007;293:H1581–H1589. doi: 10.1152/ajpheart.00278.2007
28. Arvanitis DA, Vafiadaki E, Johnson DM, Kranias EG, Sanoudou D. The histidine-rich calcium binding protein in regulation of cardiac rhythmicity. *Front Physiol*. 2018;9:1379. doi: 10.3389/fphys.2018.01379
29. Lin DJ, Lee WS, Chien YC, Chen TY, Yang KT. The link between abnormalities of calcium handling proteins and catecholaminergic polymorphic ventricular tachycardia. *Tzu Chi Med J*. 2021;33:323–331. doi: 10.4103/tcmj.tcmj_288_20
30. Pollak AJ, Haghighi K, Kunduri S, Arvanitis DA, Bidwell PA, Liu GS, Singh VP, Gonzalez DJ, Sanoudou D, Wiley SE, et al. Phosphorylation of serine96 of histidine-rich calcium-binding protein by the Fam20C kinase functions to prevent cardiac arrhythmia. *Proc Natl Acad Sci USA*. 2017;114:9098–9103. doi: 10.1073/pnas.1706441114
31. Valle G, Boncompagni S, Sacchetto R, Protasi F, Volpe P. Post-natal heart adaptation in a knock-in mouse model of calsequestrin 2-linked

recessive catecholaminergic polymorphic ventricular tachycardia. *Exp Cell Res*. 2014;321:178–189. doi: 10.1016/j.yexcr.2013.12.014
32. Hinte F, Müller J, Brune W. Viral mediated tethering to SEL1L facilitates ER-associated degradation of IRE1. *J Virol*. 2021;95:e01990-20. doi: 10.1128/JVI.01990-20
33. Li Y, Li S, Wu H. Ubiquitination-proteasome system (UPS) and autophagy two main protein degradation machineries in response to cell stress. *Cells*. 2022;11:851. doi: 10.3390/cells11050851
34. Lindholm D, Korhonen L, Eriksson O, Kõks S. Recent insights into the role of unfolded protein response in ER stress in health and disease. *Front Cell Dev Biol*. 2017;5:48. doi: 10.3389/fcell.2017.00048
35. Hwang J, Qi L. Quality control in the endoplasmic reticulum: crosstalk between ERAD and UPR pathways. *Trends Biochem Sci*. 2018;43:593–605. doi: 10.1016/j.tibs.2018.06.005
36. Song S, Tan J, Miao Y, Zhang Q. Crosstalk of ER stress-mediated autophagy and ER-phagy: involvement of UPR and the core autophagy machinery. *J Cell Physiol*. 2018;233:3867–3874. doi: 10.1002/jcp.26137
37. Patterson C, Portbury AL, Schisler JC, Willis MS. Tear me down: role of calpain in the development of cardiac ventricular hypertrophy. *Circ Res*. 2011;109:453–462. doi: 10.1161/CIRCRESAHA.110.239749
38. Ono Y, Saido TC, Sorimachi H. Calpain research for drug discovery: challenges and potential. *Nat Rev Drug Discov*. 2016;15:854–876. doi: 10.1038/nrd.2016.212
39. Sandmann S, Prenzel F, Shaw L, Schauer R, Unger T. Activity profile of calpains I and II in chronically infarcted rat myocardium—influence of the calpain inhibitor CAL 9961. *Br J Pharmacol*. 2002;135:1951–1958. doi: 10.1038/sj.bjp.0704661
40. Letavernier E, Zafrani L, Perez J, Letavernier B, Haymann JP, Baud L. The role of calpains in myocardial remodelling and heart failure. *Cardiovasc Res*. 2012;96:38–45. doi: 10.1093/cvr/cvs099
41. Ye T, Wang Q, Zhang Y, Song X, Yang D, Li D, Li D, Su L, Yang Y, Ma S. Over-expression of calpastatin inhibits calpain activation and attenuates post-infarction myocardial remodeling. *PLoS One*. 2015;10:e0120178. doi: 10.1371/journal.pone.0120178
42. Poncelas M, Inserte J, Aluja D, Hernando V, Vilardosa U, Garcia-Dorado D. Delayed, oral pharmacological inhibition of calpains attenuates adverse post-infarction remodelling. *Cardiovasc Res*. 2017;113:950–961. doi: 10.1093/cvr/cvx073
43. Hamilton S, Terentyeva R, Veress R, Perger F, Nichtova Z, Bannister M, Wang J, Quiggle S, Battershell R, Gorr MW, et al. Increased intermembrane space [Ca^{2+}] drives mitochondrial structural damage in CPVT. *Circ Res*. 2025;137:1385–1403. doi: 10.1161/CIRCRESAHA.125.326841
44. Chopra N, Kannankeril PJ, Yang T, Hlaing T, Holinstat I, Ettensohn K, Pfeifer K, Akin B, Jones LR, Franzini-Armstrong C, et al. Modest reductions of cardiac calsequestrin increase sarcoplasmic reticulum Ca^{2+} leak independent of luminal Ca^{2+} and trigger ventricular arrhythmias in mice. *Circ Res*. 2007;101:617–626. doi: 10.1161/CIRCRESAHA.107.157552
45. Gelman A. Prior distributions for variance parameters in hierarchical models (comment on article by Browne and Draper). *Bayesian Anal*. 2006;1:515–534. doi: 10.1214/06-ba117a
46. Bürkner PC. brms: an R package for Bayesian multilevel models using *Stan*. *J Stat Softw*. 2017;80. doi: 10.18637/jss.v080.i01
47. Bonzon-Kulichenko E, Camafeita E, López JA, Gómez-Serrano M, Jorge I, Calvo E, Núñez E, Trevisan-Herraz M, Bagwan N, Bárcena JA, et al. Improved integrative analysis of the thiol redox proteome using filter-aided sample preparation. *J Proteomics*. 2020;214:103624. doi: 10.1016/j.jprot.2019.103624
48. Bonzon-Kulichenko E, Garcia-Marques F, Trevisan-Herraz M, Vázquez J. Revisiting peptide identification by high-accuracy mass spectrometry: problems associated with the use of narrow mass precursor windows. *J Proteome Res*. 2015;14:700–710. doi: 10.1021/pr5007284
49. Navarro P, Trevisan-Herraz M, Bonzon-Kulichenko E, Núñez E, Martínez-Acedo P, Pérez-Hernández D, Jorge I, Mesa R, Calvo E, Carrascal M, et al. General statistical framework for quantitative proteomics by stable isotope labeling. *J Proteome Res*. 2014;13:1234–1247. doi: 10.1021/pr4006958
50. García-Marqués F, Trevisan-Herraz M, Martínez-Martínez S, Camafeita E, Jorge I, Lopez JA, Méndez-Barbero N, Méndez-Ferrer S, Del Pozo MA, Ibáñez B, et al. A novel systems-biology algorithm for the analysis of coordinated protein responses using quantitative proteomics. *Mol Cell Proteomics*. 2016;15:1740–1760. doi: 10.1074/mcp.M115.055905
51. Trevisan-Herraz M, Bagwan N, García-Marqués F, Rodriguez JM, Jorge I, Ezkurdia I, Bonzon-Kulichenko E, Vázquez J. SanXoT: a modular and versatile package for the quantitative analysis of high-throughput proteomics experiments. *Bioinformatics*. 2019;35:1594–1596. doi: 10.1093/bioinformatics/bty815
52. Carbon S, Douglass E, Dunn N, Good B, Harris NL, Lewis SE, Mungall CJ, Basu S, Chisholm RL, Dodson RJ, et al. The Gene Ontology Resource: 20 years and still going strong. *Nucleic Acids Res*. 2019;47:D330–D338. doi: 10.1093/nar/gky1055

Downloaded from http://ahajournals.org by on November 5, 2026